

## 2 **Construction of Green's function using null-field integral** 3 **approach for Laplace problems with circular boundaries**

4 **Jeng-Tzong Chen<sup>1</sup>, Jia-Nan Ke and Huan-Zhen Liao**

5 **Abstract:** A null-field approach is employed to derive the Green's function for  
6 boundary value problems stated for the Laplace equation with circular boundaries.  
7 The kernel function and boundary density are expanded by using the degenerate  
8 kernel and Fourier series, respectively. Series-form Green's function for interior  
9 and exterior problems of circular boundary are derived and plotted in a good agree-  
10 ment with the closed-form solution. The Poisson integral formula is extended to  
11 an annular case from a circle. Not only an eccentric ring but also a half-plane  
12 problem with an aperture are demonstrated to see the validity of the present ap-  
13 proach. Besides, a half-plane problem with a circular hole subject to Dirichlet  
14 and Robin boundary condition and a half-plane problem with a circular hole and a  
15 semi-circular inclusion are solved. Good agreement is made after comparing with  
16 the Melnikov's results.

17 **Keywords:** degenerate kernel, Fourier series, Green's function, null-field approach  
18 and Poisson integral formula.

### 19 **1 Introduction**

20 Green's function has been studied and applied in many fields by mathematicians as  
21 well as engineers [Jaswon and Symm (1977); Melnikov (1977); Yang and Tewary  
22 (2008); Yang, Wong and Qu (2008)]. According to the superposition principle, the  
23 problems with distributed loading can be easily solved. The main difference from  
24 the fundamental solution (free-space Green's function) is that it not only satisfies  
25 the governing equation with a concentrated source but also matches the bound-  
26 ary condition of bounded domain. Poisson integral formula was constructed after  
27 the special Green's function is obtained. It is well known that the kernel function  
28 in the Poisson integral formula is the normal derivative of the Green's function  
29 for the Dirichlet problem of a circle. For deriving the Green's function, Thompson  
30 [Thomson (1848)] proposed the concept of reciprocal radii to find the image source

---

<sup>1</sup> Department of Harbor and River Engineering, National Taiwan Ocean University, Keelung, Taiwan

31 to satisfy the homogeneous Dirichlet boundary condition. A Green function for  
 32 a continuously non-homogeneous saturated media has been presented [Seyrafiyan,  
 33 Gatmiri and Noorzad (2006)]. On the other hand, Chen and Wu [Chen and Wu  
 34 (2006)] proposed an alternative way to find the location of image through the de-  
 35 generate kernel. For complicated domain, closed-form Green's function as well  
 36 as series form is not easy to obtain. Analytical Green's functions have been pre-  
 37 sented for only a few configurations in two-dimensional applications and require  
 38 complex variable theory. Numerical Green's function has received attention from  
 39 BEM researchers by Telles et al. [Telles, Castor and Guimaraes (1995); Guimaraes  
 40 and Telles (2000); Ang and Telles (2004); Melnikov (2001)]. Melnikov used the  
 41 method of modified potential (MMP) to calculate the Green's function of eccen-  
 42 tric ring and half-plane problems with a circular boundary. Boley [Boley (1956)]  
 43 analytically constructed the Green's function by using successive approximation.  
 44 Adewale [Adewale (2006)] proposed an analytical solution for an annular plate  
 45 subjected to a concentrated load which also belongs to the Green's function.

46 In this paper, we focus on the null-field approach to determine the Green's function  
 47 for problems with circular boundary. Green's function for annular, eccentric case  
 48 and half-plane problems with a circular hole or an aperture and a semi-circular  
 49 inclusion are found semi-analytically. Analytical and semi-analytical solutions for  
 50 the annular case are checked by each other. The results of eccentric case and half-  
 51 plane problems with a circular hole or an aperture and a semi-circular inclusion are  
 52 compared with those by Melnikov.

## 53 2 Derivation of the Green's function for Laplace problems with circular bound- 54 aries

### 55 2.1 Problem statement and null-field integral approach to construct the Green's 56 function

For a two-dimensional problem with circular boundaries as shown in Fig. 1, the  
 Green's function satisfies

$$\nabla^2 G(x, \xi) = \delta(x - \xi), \quad x \in D, \quad (1)$$

where  $D$  is the domain and  $\delta(x - \xi)$  denotes the Dirac-delta function of source at  
 $\xi$ . For simplicity, this problem is subject to the Dirichlet boundary condition

$$G(x, \xi) = 0, \quad x \in B, \quad (2)$$

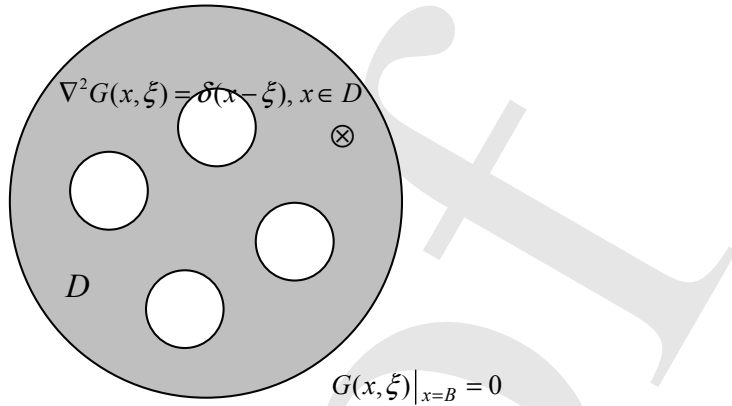


Figure 1: Green's function for Laplace problems with circular boundaries

where  $B$  is the boundary. In order to employ the Green's third identity [Rashed (2004)] as follows

$$\iint_D [u(x)\nabla^2 v(x) - v(x)\nabla^2 u(x)]dD(x) = \int_B [(u(x)\frac{\partial v(x)}{\partial n} - v(x)\frac{\partial u(x)}{\partial n})]dB(x), \quad (3)$$

we need two systems,  $u(x)$  and  $v(x)$ . We choose  $u(x)$  as  $G(x, \xi)$  and set  $v(x)$  as the fundamental solution  $U(x, s)$  such that

$$\nabla^2 U(x, s) = 2\pi\delta(x - s). \quad (4)$$

Then, we can obtain the fundamental solution as follows

$$U(s, x) = \ln r, \quad (5)$$

57 where  $r$  is the distance between  $s$  and  $x$  ( $r \equiv |x - s|$ ).

After exchanging with the variables  $x$  and  $s$ , we have

$$2\pi G(x, \xi) = \int_B T(s, x)G(s, \xi)dB(s) - \int_B U(s, x)\frac{\partial G(s, \xi)}{\partial n_s}dB(s) + U(\xi, x), \quad (6)$$

where  $T(s, x)$  is defined by

$$T(s, x) \equiv \frac{\partial U(s, x)}{\partial n_s}, \quad (7)$$

in which  $n_s$  denotes the outward normal vector at the source point  $s$ . To solve the above equation, we utilize the null-field integral equation to derive the Green's function. To solve the unknown boundary density  $\partial G/\partial n_s$ , the field point  $x$  is located outside the domain to yield the null-field integral equation as shown below:

$$0 = \int_B T(s, x)G(s, \xi)dB(s) - \int_B U(s, x)\frac{\partial G(s, \xi)}{\partial n_s}dB(s) + U(\xi, x), \quad x \in D^c \quad (8)$$

58 where  $D^c$  is the complementary domain. By using the degenerate kernels, the BIE  
59 for the "boundary point" can be easily derived through the null-field integral equa-  
60 tion by exactly collocating  $x$  on  $B$  in Eq. (8) [Chen, Shen and Chen (2006)].

## 61 2.2 Expansion of kernel function and boundary density

Based on the separable property, the kernel function  $U(s, x)$  can be expanded into series form by separating the field point  $x(\rho, \phi)$  and source point  $s(R, \theta)$  in the polar coordinate:

$$U(s, x) = \begin{cases} U^i(R, \theta; \rho, \phi) = \ln R - \sum_{m=1}^{\infty} \frac{1}{m} \left(\frac{\rho}{R}\right)^m \cos m(\theta - \phi), & R \geq \rho \\ U^e(R, \theta; \rho, \phi) = \ln \rho - \sum_{m=1}^{\infty} \frac{1}{m} \left(\frac{R}{\rho}\right)^m \cos m(\theta - \phi), & \rho > R \end{cases} \quad (9)$$

It is noted that the leading term and the numerator in the above expansion involve the larger argument to ensure the log singularity and the series convergence, respectively. According to the definition of  $T(s, x)$  in Eq. (7), we have

$$T(s, x) = \begin{cases} T^i(R, \theta; \rho, \phi) = \frac{1}{R} + \sum_{m=1}^{\infty} \left(\frac{\rho^m}{R^{m+1}}\right) \cos m(\theta - \phi), & R > \rho \\ T^e(R, \theta; \rho, \phi) = - \sum_{m=1}^{\infty} \left(\frac{R^{m-1}}{\rho^m}\right) \cos m(\theta - \phi), & \rho > R \end{cases} \quad (10)$$

The unknown boundary densities can be represented by using the Fourier series as shown below:

$$G(s_k, \xi) = a_0^k + \sum_{n=1}^{\infty} (a_n^k \cos n\theta_k + b_n^k \sin n\theta_k), \quad s_k \in B_k, k = 1, 2, \dots, N, \quad (11)$$

$$\frac{\partial G(s_k, \xi)}{\partial n_s} = p_0^k + \sum_{n=1}^{\infty} (p_n^k \cos n\theta_k + q_n^k \sin n\theta_k), \quad s_k \in B_k, k = 1, 2, \dots, N, \quad (12)$$

62 where  $N$  is the number of circular boundaries. In real computation, the finite  $M$   
63 terms for expansion of kernel and boundary density are adopted.

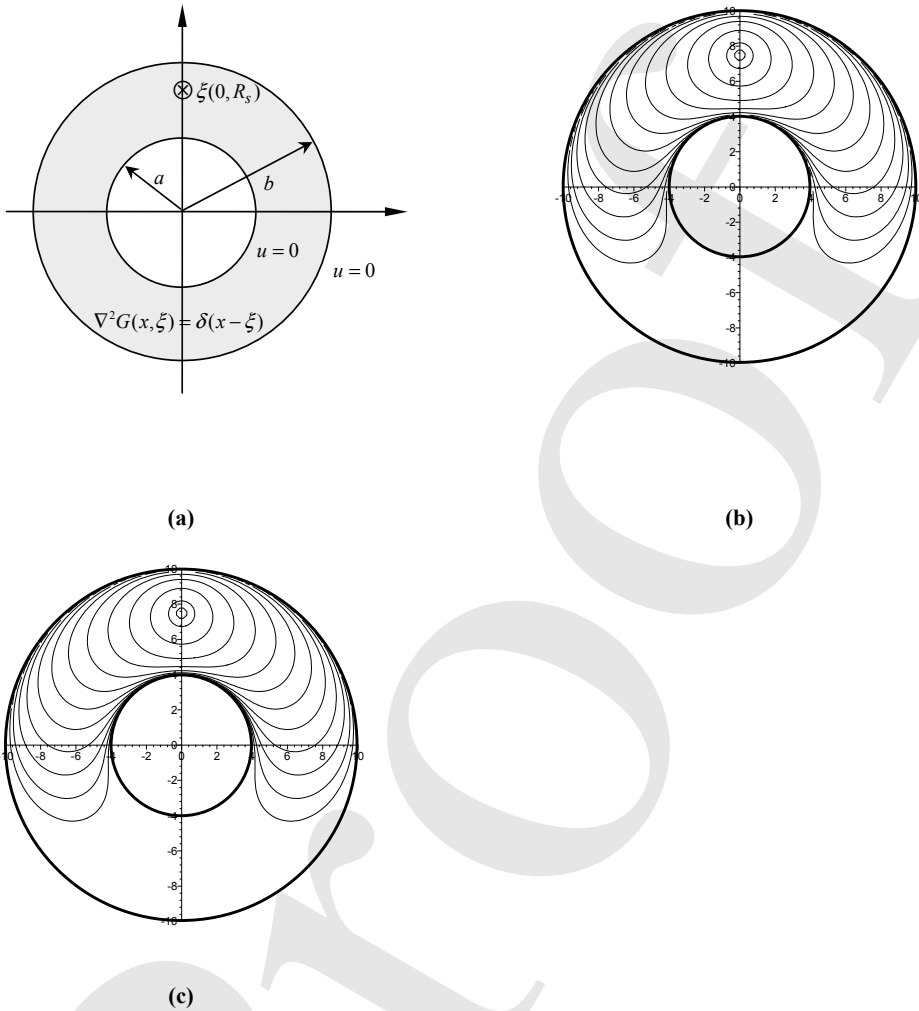


Figure 2: (a): Green's function for annular case; (b): Green's function for annular case (analytical solution,  $M=50$ ); (c): Green's function for annular case (semi-analytical solution,  $M=50$ )

64 **3 Series representation for the Green's function of annular case**

For the annular case as shown in Fig. 2(a) subject to the Dirichlet boundary condition, the unknown Fourier series can be analytically derived. By collocating  $x$  on

$(b^+, \phi)$  and  $(a^-, \phi)$ , the null-field equations yield

$$0 = (1 - 2\pi b p_0 - 2\pi a \bar{p}_0) \ln b - \sum_{m=1}^{\infty} \frac{1}{m} \{ [b\pi p_m + a\pi \left(\frac{a}{b}\right)^m \bar{p}_m + \left(\frac{R_s}{b}\right)^m \cos m\theta_s] \cos m\phi + [b\pi q_m + a\pi \left(\frac{a}{b}\right)^m \bar{q}_m + \left(\frac{R_s}{b}\right)^m \sin m\theta_s] \sin m\phi \}, x \rightarrow (b^+, \phi) \quad (13)$$

$$0 = (\ln R_s - 2\pi b \ln b p_0 - 2\pi a \ln a \bar{p}_0) - \sum_{m=1}^{\infty} \frac{1}{m} \{ [b\pi \left(\frac{a}{b}\right)^m p_m + a\pi \bar{p}_m + \left(\frac{a}{R_s}\right)^m \cos m\theta_s] \cos m\phi + [b\pi \left(\frac{a}{b}\right)^m q_m + a\pi \bar{q}_m + \left(\frac{a}{R_s}\right)^m \sin m\theta_s] \sin m\phi \}, x \rightarrow (a^-, \phi) \quad (14)$$

where  $a$  and  $b$  are the inner and outer radii, respectively. For the Dirichlet case, the explicit form for the unknown Fourier series can be obtained as

$$\left\{ \begin{matrix} p_0 \\ \bar{p}_0 \end{matrix} \right\} = \left\{ \begin{matrix} \frac{\ln a - \ln R_s}{2\pi b (\ln a - \ln b)} \\ \frac{\ln b - \ln R_s}{2\pi a (\ln b - \ln a)} \end{matrix} \right\} \quad (15)$$

$$\left\{ \begin{matrix} p_m \\ \bar{p}_m \end{matrix} \right\} = \left\{ \begin{matrix} \frac{b^{m-1} \cos m\theta_s [b^m \left(\frac{R_s}{b}\right)^m - a^m \left(\frac{a}{R_s}\right)^m]}{(b^{2m} - a^{2m})\pi} \\ \frac{b^m \cos m\theta_s [b^m \left(\frac{a}{R_s}\right)^m - a^m \left(\frac{R_s}{b}\right)^m]}{a(b^{2m} - a^{2m})\pi} \end{matrix} \right\} \quad (16)$$

$$\left\{ \begin{matrix} q_m \\ \bar{q}_m \end{matrix} \right\} = \left\{ \begin{matrix} \frac{b^{m-1} \sin m\theta_s [b^m \left(\frac{R_s}{b}\right)^m - a^m \left(\frac{a}{R_s}\right)^m]}{(b^{2m} - a^{2m})\pi} \\ \frac{b^m \sin m\theta_s [b^m \left(\frac{a}{R_s}\right)^m - a^m \left(\frac{R_s}{b}\right)^m]}{a(b^{2m} - a^{2m})\pi} \end{matrix} \right\} \quad (17)$$

where  $p_m$ ,  $q_m$ ,  $\bar{p}_m$  and  $\bar{q}_m$  are the Fourier coefficients of boundary densities for normal flux as shown below:

$$t(s) = \sum_{m=0}^{\infty} (\bar{p}_m \cos m\theta + \bar{q}_m \sin m\theta), \quad s \in \text{inner boundary} \quad (18)$$

$$t(s) = \sum_{m=0}^{\infty} (p_m \cos m\theta + q_m \sin m\theta), \quad s \in \text{outer boundary} \quad (19)$$

By substituting all the boundary densities into the integral representation for the domain point, we have the series-form Green's function as shown below:

$$\begin{aligned}
 G(x, \xi) = & -(b \ln b p_0 + a \ln \rho \bar{p}_0) \\
 & + \sum_{m=1}^{\infty} \frac{1}{2m} \left\{ \left[ b \left( \frac{\rho}{b} \right)^m p_m + a \left( \frac{a}{\rho} \right)^m \bar{p}_m \right] \cos m\phi \right. \\
 & \quad \left. + \left[ b \left( \frac{\rho}{b} \right)^m q_m + a \left( \frac{a}{\rho} \right)^m \bar{q}_m \right] \sin m\phi \right\} + \frac{\ln|x - \xi|}{2\pi}, \quad a \leq \rho \leq b \quad (20)
 \end{aligned}$$

If we expand the function, we have

$$\begin{aligned}
 G(x, \xi) = & -(b \ln b p_0 + a \ln \rho \bar{p}_0 - \frac{\ln \rho}{2\pi}) \\
 & + \sum_{m=1}^{\infty} \frac{1}{2m} \left\{ \left[ b \left( \frac{\rho}{b} \right)^m p_m + a \left( \frac{a}{\rho} \right)^m \bar{p}_m - \left( \frac{R_s}{\rho} \right)^m \frac{\cos m\theta_s}{\pi} \right] \cos m\phi \right. \\
 & \quad \left. + \left[ b \left( \frac{\rho}{b} \right)^m q_m + a \left( \frac{a}{\rho} \right)^m \bar{q}_m - \left( \frac{R_s}{\rho} \right)^m \frac{\sin m\theta_s}{\pi} \right] \sin m\phi \right\}, \quad R_s \leq \rho \leq b \quad (21)
 \end{aligned}$$

$$\begin{aligned}
 G(x, \xi) = & -(b \ln b p_0 + a \ln \rho \bar{p}_0 - \frac{\ln R_s}{2\pi}) \\
 & + \sum_{m=1}^{\infty} \frac{1}{2m} \left\{ \left[ b \left( \frac{\rho}{b} \right)^m p_m + a \left( \frac{a}{\rho} \right)^m \bar{p}_m - \left( \frac{\rho}{R_s} \right)^m \frac{\cos m\theta_s}{\pi} \right] \cos m\phi \right. \\
 & \quad \left. + \left[ b \left( \frac{\rho}{b} \right)^m q_m + a \left( \frac{a}{\rho} \right)^m \bar{q}_m - \left( \frac{\rho}{R_s} \right)^m \frac{\sin m\theta_s}{\pi} \right] \sin m\phi \right\}, \quad a \leq \rho \leq R_s \quad (22)
 \end{aligned}$$

Also, two limiting cases are our concern. One is the interior case of  $a$  to zero and the other is the exterior case of  $b$  to infinity. Now we move to solve the solution  $w(x)$  for the following partial differential equation

$$\nabla^2 w(x) = 0, \quad x \in D, \quad (23)$$

subject to the following Dirichlet boundary condition

$$w(x) = f(x), \quad x \in \text{inner boundary } B_1 \quad (24)$$

$$w(x) = g(x), \quad x \in \text{outer boundary } B_2 \quad (25)$$

To extend the Poisson integral formula to an annular case for Eq. (20) subject to BCs of Eqs. (24) and (25), we have

$$2\pi w(x) = \int_{B_1+B_2} \frac{\partial G(s, x)}{\partial n_s} w(s) dB(s) \quad (26)$$

65 where  $G(s, x)$  is the derived Green's function of Eq. (20). Equation (26) indicates  
 66 the representation for the solution in terms of general Poisson integral formula.

67 Although the series-form Green's function for an annular case is derived analyti-  
 68 cally in the section, general Green's functions can be solved semi-analytically as  
 69 shown in the following section.

#### 70 4 Linear algebraic equation

By moving the null-field point  $x_j$  to the  $j$ th circular boundary in the limit sense for Eq. (8), we have the linear algebraic equation

$$[\mathbf{U}]\{\mathbf{t}\} = [\mathbf{T}]\{\mathbf{u}\} + \{\mathbf{b}\}, \quad (27)$$

where  $\{\mathbf{b}\}$  is the vector due to the source of Green's function,  $[\mathbf{U}]$  and  $[\mathbf{T}]$  are the influence matrices with a dimension of  $(N + 1)(2M + 1)$  by  $(N + 1)(2M + 1)$ ,  $\{\mathbf{u}\}$  and  $\{\mathbf{t}\}$  denote the column vectors of Fourier coefficients with a dimension of  $(N + 1)(2M + 1)$  by 1 in which  $[\mathbf{U}]$ ,  $[\mathbf{T}]$ ,  $\{\mathbf{u}\}$ ,  $\{\mathbf{t}\}$  and  $\{\mathbf{b}\}$  can be defined as follows:

$$[\mathbf{U}] = \begin{bmatrix} \mathbf{U}_{00} & \mathbf{U}_{01} & \cdots & \mathbf{U}_{0N} \\ \mathbf{U}_{10} & \mathbf{U}_{11} & \cdots & \mathbf{U}_{1N} \\ \vdots & \vdots & \ddots & \vdots \\ \mathbf{U}_{N0} & \mathbf{U}_{N1} & \cdots & \mathbf{U}_{NN} \end{bmatrix}, \quad [\mathbf{T}] = \begin{bmatrix} \mathbf{T}_{00} & \mathbf{T}_{01} & \cdots & \mathbf{T}_{0N} \\ \mathbf{T}_{10} & \mathbf{T}_{11} & \cdots & \mathbf{T}_{1N} \\ \vdots & \vdots & \ddots & \vdots \\ \mathbf{T}_{N0} & \mathbf{T}_{N1} & \cdots & \mathbf{T}_{NN} \end{bmatrix}, \quad (28)$$

$$\{\mathbf{u}\} = \begin{pmatrix} \mathbf{u}_0 \\ \mathbf{u}_1 \\ \mathbf{u}_2 \\ \vdots \\ \mathbf{u}_N \end{pmatrix}, \quad \{\mathbf{t}\} = \begin{pmatrix} \mathbf{t}_0 \\ \mathbf{t}_1 \\ \mathbf{t}_2 \\ \vdots \\ \mathbf{t}_N \end{pmatrix}, \quad \{\mathbf{b}\} = \begin{pmatrix} \mathbf{b}_0 \\ \mathbf{b}_1 \\ \mathbf{b}_2 \\ \vdots \\ \mathbf{b}_N \end{pmatrix} \quad (29)$$

where the vectors  $\{\mathbf{u}_k\}$  and  $\{\mathbf{t}_k\}$  are in the form of  $\{a_0^k \ a_1^k \ b_1^k \ \cdots \ a_M^k \ b_M^k\}^T$  and  $\{p_0^k \ p_1^k \ q_1^k \ \cdots \ p_M^k \ q_M^k\}^T$  respectively; the first subscript "j" ( $j = 0, 1, 2, \dots, N$ ) in  $[\mathbf{U}_{jk}]$  and  $[\mathbf{T}_{jk}]$  denotes the index of the  $j$ th circle where the collocation point is located and the second subscript "k" ( $k = 0, 1, 2, \dots, N$ ) denotes the index of the  $k$ th circle where boundary data  $\{\mathbf{u}_k\}$  or  $\{\mathbf{t}_k\}$  are specified,  $N$  is the number of circular holes in the domain and  $M$  indicates the truncated terms of Fourier series. The coefficient matrix of the linear algebraic system is partitioned into blocks, and each off-diagonal block corresponds to the influence matrices between two different circular cavities. The diagonal blocks are the influence matrices due to itself in each individual hole. After uniformly collocating the point along the  $k$ th circular



boundary, the submatrix can be written as

$$[\mathbf{U}_{jk}] = \begin{bmatrix} U_{jk}^{0c}(\phi_1) & U_{jk}^{1c}(\phi_1) & U_{jk}^{1s}(\phi_1) \\ U_{jk}^{0c}(\phi_2) & U_{jk}^{1c}(\phi_2) & U_{jk}^{1s}(\phi_2) \\ U_{jk}^{0c}(\phi_3) & U_{jk}^{1c}(\phi_3) & U_{jk}^{1s}(\phi_3) \\ \vdots & \vdots & \vdots \\ U_{jk}^{0c}(\phi_{2M}) & U_{jk}^{1c}(\phi_{2M}) & U_{jk}^{1s}(\phi_{2M}) \\ U_{jk}^{0c}(\phi_{2M+1}) & U_{jk}^{1c}(\phi_{2M+1}) & U_{jk}^{1s}(\phi_{2M+1}) \\ \cdots & U_{jk}^{Mc}(\phi_1) & U_{jk}^{Ms}(\phi_1) \\ \cdots & U_{jk}^{Mc}(\phi_2) & U_{jk}^{Ms}(\phi_2) \\ \cdots & U_{jk}^{Mc}(\phi_3) & U_{jk}^{Ms}(\phi_3) \\ \vdots & \vdots & \vdots \\ \cdots & U_{jk}^{Mc}(\phi_{2M}) & U_{jk}^{Ms}(\phi_{2M}) \\ \cdots & U_{jk}^{Mc}(\phi_{2M+1}) & U_{jk}^{Ms}(\phi_{2M+1}) \end{bmatrix} \quad (30)$$

$$[\mathbf{T}_{jk}] = \begin{bmatrix} T_{jk}^{0c}(\phi_1) & T_{jk}^{1c}(\phi_1) & T_{jk}^{1s}(\phi_1) \\ T_{jk}^{0c}(\phi_2) & T_{jk}^{1c}(\phi_2) & T_{jk}^{1s}(\phi_2) \\ T_{jk}^{0c}(\phi_3) & T_{jk}^{1c}(\phi_3) & T_{jk}^{1s}(\phi_3) \\ \vdots & \vdots & \vdots \\ T_{jk}^{0c}(\phi_{2M}) & T_{jk}^{1c}(\phi_{2M}) & T_{jk}^{1s}(\phi_{2M}) \\ T_{jk}^{0c}(\phi_{2M+1}) & T_{jk}^{1c}(\phi_{2M+1}) & T_{jk}^{1s}(\phi_{2M+1}) \\ \cdots & T_{jk}^{Mc}(\phi_1) & T_{jk}^{Ms}(\phi_1) \\ \cdots & T_{jk}^{Mc}(\phi_2) & T_{jk}^{Ms}(\phi_2) \\ \cdots & T_{jk}^{Mc}(\phi_3) & T_{jk}^{Ms}(\phi_3) \\ \vdots & \vdots & \vdots \\ \cdots & T_{jk}^{Mc}(\phi_{2M}) & T_{jk}^{Ms}(\phi_{2M}) \\ \cdots & T_{jk}^{Mc}(\phi_{2M+1}) & T_{jk}^{Ms}(\phi_{2M+1}) \end{bmatrix} \quad (31)$$

$$\{\mathbf{b}_j\} = \begin{bmatrix} \ln |\mathbf{x}(\rho_j, \phi_1) - \xi| \\ \ln |\mathbf{x}(\rho_j, \phi_2) - \xi| \\ \ln |\mathbf{x}(\rho_j, \phi_3) - \xi| \\ \vdots \\ \ln |\mathbf{x}(\rho_j, \phi_{2M+1}) - \xi| \end{bmatrix} \quad (32)$$

where the influence coefficients are explicitly expressed as

$$U_{jk}^{nc}(\phi_m) = \int_{B_k} U(s_k, x_m) \cos(n\theta_k) R_k d\theta_k, \quad (33)$$

$$U_{jk}^{ns}(\phi_m) = \int_{B_k} U(s_k, x_m) \sin(n\theta_k) R_k d\theta_k, \quad (34)$$

$$T_{jk}^{nc}(\phi_m) = \int_{B_k} T(s_k, x_m) \cos(n\theta_k) R_k d\theta_k, \quad (35)$$

$$T_{jk}^{ns}(\phi_m) = \int_{B_k} T(s_k, x_m) \sin(n\theta_k) R_k d\theta_k, \quad (36)$$

71 where  $n = 0, 1, 2, \dots, M$ ,  $m = 1, 2, \dots, 2M + 1$ , and  $\phi_m$  is the polar angle of  
 72 the collocating points  $x_m$  along the boundary. By rearranging the known and un-  
 73 known sets, the unknown Fourier coefficients are determined. Equation (8) can be  
 74 calculated by employing the relations of trigonometric function and the orthogonal  
 75 property in the real computation. Only the finite  $M$  terms are used in the Fourier  
 76 expansion of boundary densities and kernels. After obtaining the unknown Fourier  
 77 coefficients, we can obtain the interior potential by employing Eq. (6).

78 **5 Derivation of the Green's function with several circular holes and inclu-**  
 79 **sions**

For the problems with inclusions, we can decompose into subsystems of matrix and inclusion after one taking free body on the interface. The two systems of matrix and inclusion yield

$$[U^M] \{t^M\} = [T^M] \{u^M\} \quad (37)$$

$$[U^I] \{t^I\} = [T^I] \{u^I\} + \{b\} \quad (38)$$

where the superscripts “ $M$ ” and “ $I$ ” denote the systems of matrix and inclusion, respectively. Two constrains of continuity for the displacement and equilibrium of force are shown below:

$$\{u^M\} = \{u^I\} \quad \text{on } B_k, \quad (39)$$

$$[-\lambda_2] \{t^M\} = [\lambda_1] \{t^I\} \quad \text{on } B_k, \quad (40)$$

80 where  $\lambda_1$  and  $\lambda_2$  represent the material conductivity of inclusion and matrix, re-  
 81 spectively.

By assembling the matrices in Eqs. (37), (38), (39) and (40), we have

$$\begin{bmatrix} T^M & -U^M & 0 & 0 \\ 0 & 0 & T^I & -U^I \\ I & 0 & -I & 0 \\ 0 & -\lambda_2 & 0 & -\lambda_1 \end{bmatrix} \begin{bmatrix} u^M \\ t^M \\ u^I \\ t^I \end{bmatrix} = \begin{bmatrix} 0 \\ U(\xi, x) - U(\xi', x) \\ 0 \\ 0 \end{bmatrix} \quad (41)$$

82 The unknown coefficients in the algebraic system can be determined. Then, we can  
 83 solve the potential by Eq. (6). The half-plane problem is imbedded to a full-plane  
 84 problem through the image method. By employing the anti-symmetric property,  
 85 the boundary condition of half-plane can be satisfied through the image approach.  
 86 In the real implementation, the full-plane problem is solved, first.

## 87 **6 Illustrative examples and discussions**

88 **Case 1:** annular case (analytical solution and semi-analytical solution).

89 The influence matrix is singular for the Dirichlet problem as the radius  $b$  is one.  
 90 No matter what the null-field point collocated ( $a^-$  and  $b^+$ ) due to the property of  
 91 degenerate kernel in Eq. (9), one column of the influence matrix  $[U]$  is a zero  
 92 vector. For more detail, please find our recent work [Chen and Shen (2007)] for  
 93 eccentric Laplace problems. Another one by Liu and Lean can be consulted [Liu  
 94 and Lean (1990)]. To avoid the degenerate scale, we design the radii of inner and  
 95 outer boundaries are 4 and 10. The source of the Green's function is located on  
 96  $\xi = (0, 7.5)$ . For the annular Green's function, both the analytical solution and the  
 97 semi-analytical results are shown in Figs. 2(b) and 2(c). The analytical solution  
 98 is obtained by truncating Fourier series of fifty terms in real implementation. One  
 99 hundred and one collocation points along the inner and outer boundaries are used  
 100 in the semi-analytical approach. Good agreement is made to verify the validity of  
 101 the program using semi-analytical procedure.

102 **Case 2:** eccentric ring (semi-analytical solution).

103 Figure 3(a) depicts the Green's function of the eccentric ring. The source point is  
 104 located at  $\xi = (0, 0.75)$ . Figures 3(b) and 3(c) show the potential distribution by  
 105 using the present method and Melnikov's approach, respectively. The two radii of  
 106 inner and outer circles are  $a=0.4$  and  $b=1.0$ . The two centers of the inner and outer  
 107 circles are  $(-0.4, 0)$  and  $(0,0)$ , respectively. It is noted that outer radius of one is  
 108 a degenerate scale and needs special treatment as described in detail by Chen and  
 109 Shen. Comparison of the present results with MCP and MMP methods is shown in  
 110 Table 1. Good agreement is made.

111 **Case 3:** a half plane with an aperture (semi-analytical solution).

112 Figure 4(a) depicts the Green's function for the half plane with a hole. The source  
 113 point is located at  $\xi = (2, 1)$ . The center and radius of the aperture are  $(0, 3)$  and  
 114  $a=1.0$ . Figures 4(b) and 4(c) show the potential distribution by using the present  
 115 method and Melnikov's approach, respectively. Good agreement is made.

116 **Case 4:** a half-plane problem with a circular boundary subject to the Robin bound-  
 117 ary condition.

Table 1: Comparison of the numerical results

Field point, y	MCP			MMP			Present Method		
	Partitioning number, k [Melnikov and Melnikov (2001)]								
	10	20	50	10	20	50	10	20	50
0	0.000280	0.000128	0.000067	0.000107	0.000049	0.000032	0.000000	0.000000	0.000000
0.2	0.010667	0.010712	0.010781	0.010700	0.010779	0.010798	0.010832	0.010832	0.010832
0.4	0.062359	0.062411	0.062443	0.062407	0.062435	0.062448	0.062458	0.062462	0.062462
0.6	0.177534	0.177574	0.177585	0.177583	0.177590	0.177593	0.177597	0.177596	0.177596
0.8	0.317893	0.317902	0.317911	0.317907	0.317913	0.317914	0.318032	0.317915	0.317915
1.0	0.000014	0.000006	0.000002	0.000000	0.000000	0.000000	0.002014	0.000064	0.000000

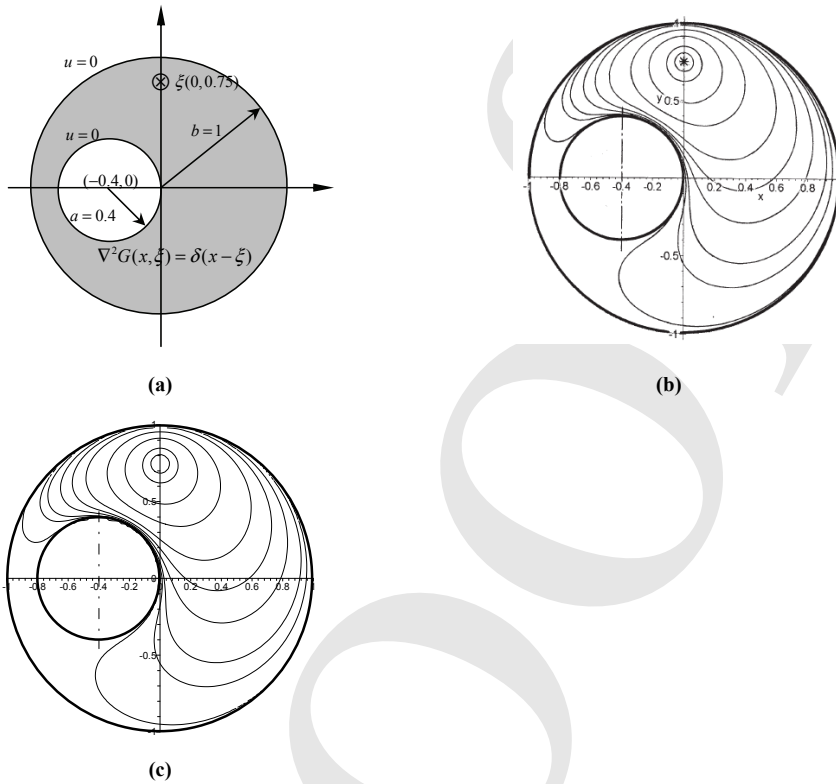


Figure 3: (a): Green's function for the eccentric ring; (b): Melnikov's method [Melnikov and Melnikov (2001)]; (c): Present method (M=50)

118 A half-plane problem with an aperture is considered. The governing equation and  
 119 boundary condition are shown in Fig. 5(a). The center and radius of the aperture  
 120 are  $(2, 2)$  and  $a=1.0$ , respectively. The Robin condition is  $t = -2u$  imposed on the  
 121 aperture. The concentrated source is located at  $(0, 3.5)$ . Figures 5(b) and 5(c) show  
 122 the potential distribution by using the present method and Melnikov's approach,  
 123 respectively. Good agreement is obtained.

124 **Case 5:** a half plane problem with a hole and an inclusion.

125 A half-plane problem with a circular hole and a half-circular inclusion are consid-  
 126 ered as composed of two regions  $D_1 = \{0 < r < 1, 0 < \varphi < \pi\}$  and  $D_2 = \{1 < r <$   
 127  $\infty, 0 < \varphi < \pi\}$  filled in with different materials ( $\lambda = \lambda_2/\lambda_1 = 0.1$ ). The governing  
 128 equation and boundary condition are shown in Fig. 6(a). The center and radius of  
 129 the aperture are  $(r, \varphi; 1.4, \pi/3)$  and  $a_2 = 0.4$ , respectively. The concentrated source

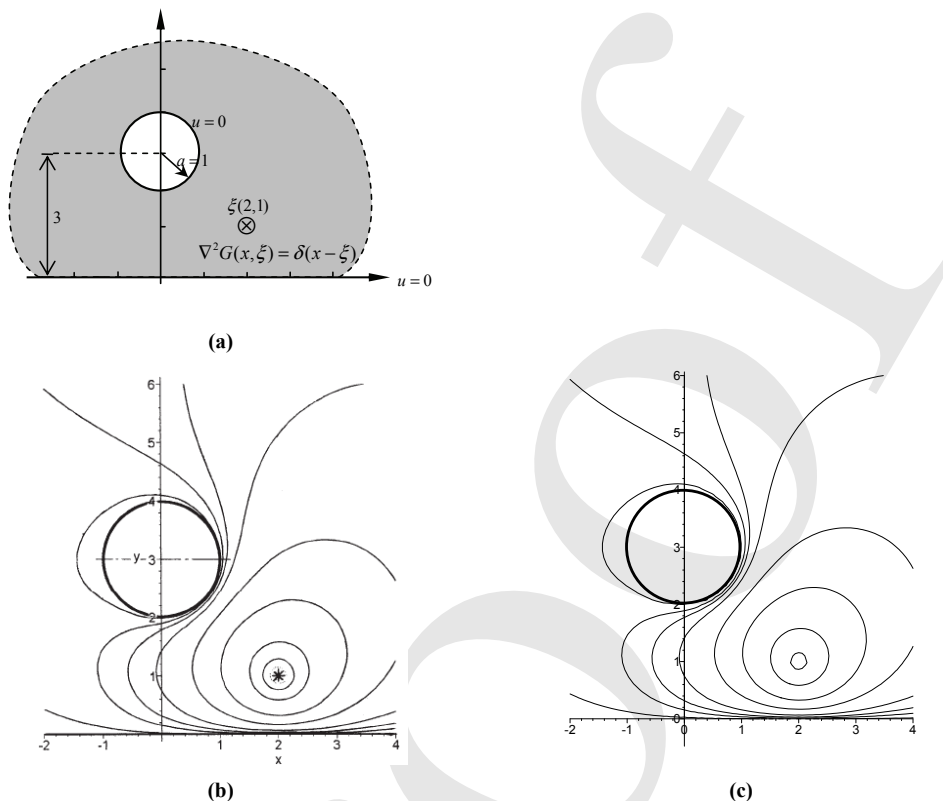


Figure 4: (a): Green's function for the half-plane with an aperture; (b): Melnikov's method [Melnikov and Melnikov (2001)]; (c): Present method (M=50)

130 is located at  $(r, \varphi; 0.5, \pi/3)$ . Figures 6(b) and 6(c) show the potential distribution by  
 131 using the present method and Melnikov's approach, respectively. Good agreement  
 132 is also made.

### 133 7 Concluding remarks

134 For the Green's function with circular boundaries, we have proposed a semi-analytical  
 135 approach to construct the Green's function by using degenerate kernels and Fourier  
 136 series. The series-form Green's function for annular Dirichlet problem is derived  
 137 which can extend the Poisson integral formula from a circle to an annular case.  
 138 Several examples, including the annular, eccentric cases and half plane problems  
 139 with circular holes and inclusions, were demonstrated to check the validity of the  
 140 present formulation. Our advantages are five folds: (1) mesh-free generation (2)

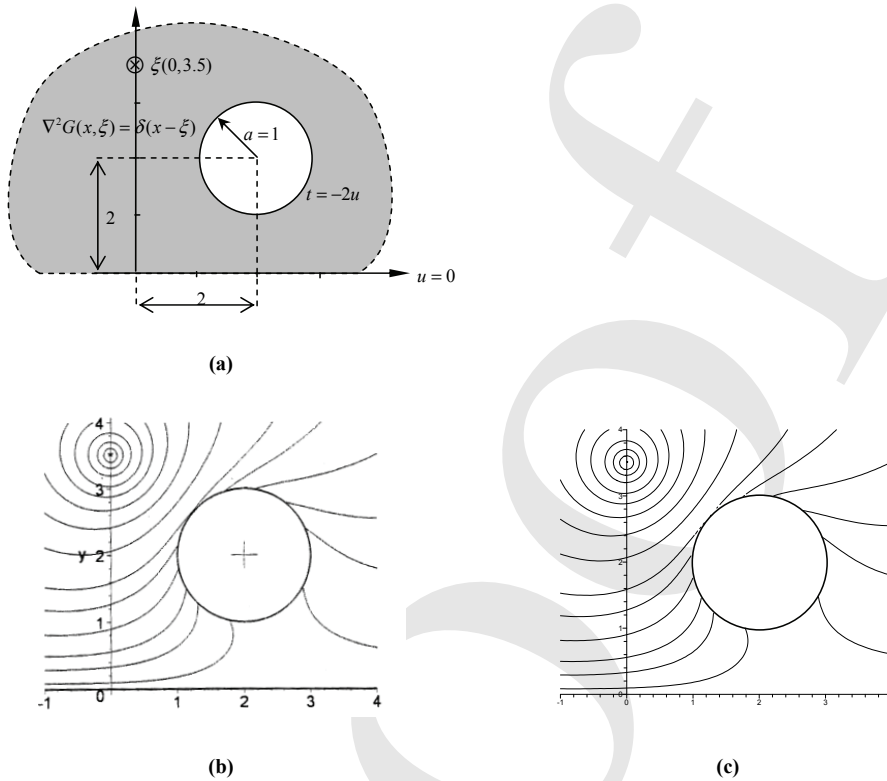


Figure 5: (a): Green's function for the half-plane problem with Robin boundary condition; (b): Contour plot by using Melnikov's approach [Melnikov and Melnikov (2006)]; (c): Contour plot by using the null-field integral equation approach (M=50)

141 well-posed model (3) principal value free (4) elimination of boundary-layer effect  
 142 (5) exponential convergence. A general-purpose program to construct the Green's  
 143 function for Laplace problems with circular boundaries of arbitrary number, radius  
 144 and location was implemented. Extension to construct the Green's functions for  
 145 Laplace problems with circular boundaries is straightforward without any difficulty.

#### 146 References

- 147 **Adewale, A. O.** (2006): Isotropic clamped-free thin annular plate subjected to a  
 148 concentrated load. *ASME, J. Appl. Mech.*, vol.73, no.4, pp. 658-663.  
 149 **Ang, W. T.; Telles, J. C. F.** (2004): A numerical Green's function for multiple

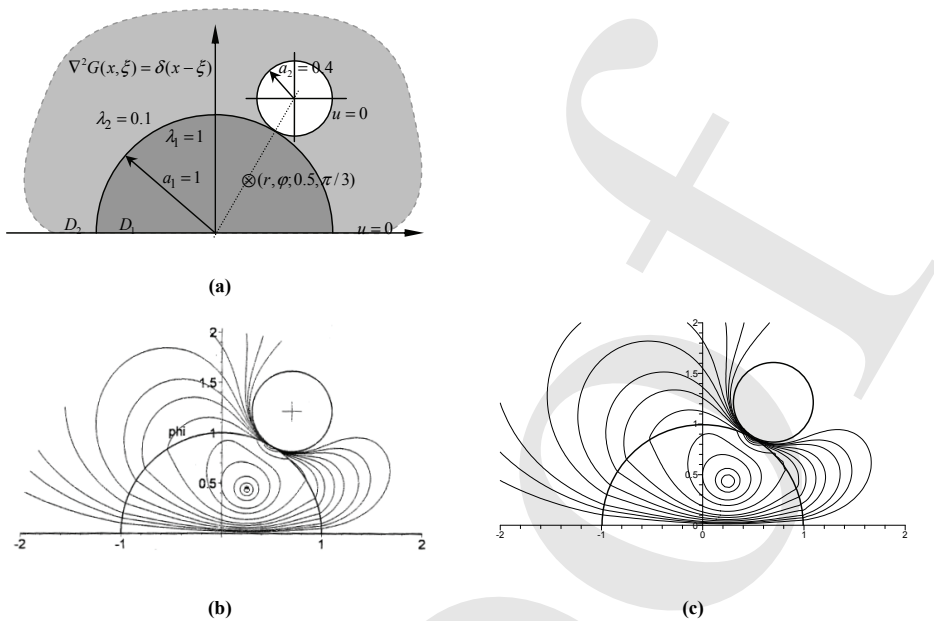


Figure 6: (a): Problem sketch of half-plane problem with a circular hole and a semi-circular inclusion; (b): Contour plot by using Melnikov's method approach [Melnikov and Melnikov (2006)]; (c): Contour plot by using the null-field integral equation approach ( $M=50$ )

150 cracks in anisotropic bodies. *Journal of Engineering Mathematics*, vol. 49, pp.  
 151 197-207.

152 **Boley, B. A.** (1956): A method for the construction of Green's functions. *Quarterly*  
 153 *of Applied Mathematics*, vol. 14, pp. 249-257.

154 **Chen, J. T.; Shen, W. C.; Chen, P. Y.** (2006): Analysis of circular torsion bar with  
 155 circular holes using null-field approach. *CMES: Computer Modeling in Engineer-*  
 156 *ing Science*, vol. 12 (2), pp. 109-119.

157 **Chen, J. T.; Shen, W. C.** (2007): Degenerate scale for multiply connected Laplace  
 158 problems. *Mechanics Research Communications*, vol. 34, pp. 69-77.

159 **Chen, J. T.; Wu, C. S.** (2006): Alternative derivations for the Poisson integral  
 160 formula. *International Journal of Mathematical Education in Science and Tech-*  
 161 *nology*, vol. 37, pp. 165-185.

162 **Guimaraes, S.; Telles, J. C. F.** (2000): General application of numerical Green's



- 163 functions for SIF computations with boundary elements. *CMES: Computer Mod-*  
164 *eling in Engineering & Sciences*, vol. 1, no. 3, pp. 131-139.
- 165 **Jaswon, M. A.; Symm, G. T.** (1977): Integral equation methods in potential theory  
166 and electrostatics. Academic Press, New York.
- 167 **Liu, P.-L. F.; Lean, M. H.** (1990): A note on  $\Gamma$ -contours in the integral equation  
168 formulation for a multi-connected region. In: Grilli, S., Brebbia, C. A., Cheng,  
169 A. H. D. (Eds.), *Computational Engineering with Boundary Elements*, vol. 1, pp.  
170 295-302.
- 171 **Melnikov, Y. A.** (1977): Some application of the Greens' function method in me-  
172 chanics. *Int. J. Solids Structures*, vol. 13, pp. 1045-1058.
- 173 **Melnikov, Y. A.; Melnikov, M. Y.** (2001): Modified potential as a tool for com-  
174 puting Green's functions in continuum mechanics. *CMES: Computer Modeling in*  
175 *Engineering & Sciences*, vol. 2, pp. 291-305.
- 176 **Melnikov, Y. A.; Melnikov, M. Y.** (2006): Green's functions for mixed bound-  
177 ary value problems in regions of irregular shape. *Electronic Journal of Boundary*  
178 *Elements*, vol. 4, pp. 82-104.
- 179 **Rashed, Y. F.** (2004): Green's first identity method for boundary-only solution of  
180 self-weight in BEM formulation for thick slabs. *CMC: Computers, Materials &*  
181 *Continua*, vol. 1, no. 4, pp. 319-326.
- 182 **Seyrafan, S.; Gatmiri, B.; Noorzad, A.** (2006): Green functions for a contin-  
183 uously non-homogeneous saturated media. *CMES: Computer Modeling in Engi-*  
184 *neering & Sciences*, vol. 15, no. 2, pp. 115-126.
- 185 **Telles, J. C. F.; Castor, G. S.; Guimaraes, S.** (1995): Numerical Green's func-  
186 tion approach for boundary elements applied to fracture mechanics. *International*  
187 *Journal for Numerical Methods in Engineering*, vol. 38, no. 19, pp. 3259-3274.
- 188 **Thomson, W.** (1848): Maxwell in his treatise, vol. I., Chap. XI, quotes a paper in  
189 the Cambridge and Dublin Math. Journ. of 1848.
- 190 **Yang, B.; Tewary, V. K.** (2008): Green's function for multilayers with interfacial  
191 membrane and flexural rigidities. *CMC: Computers Materials & Continua*, vol. 8,  
192 no. 1, pp. 23-31.
- 193 **Yang, B.; Wong, S. C.; Qu, S.;** (2008): A micromechanics analysis of nanoscale  
194 graphite platelet-reinforced epoxy using defect Green's function. *CMES: Computer*  
195 *Modeling in Engineering & Sciences*, vol. 24, no. 2-3, pp. 81-93.

Proof